

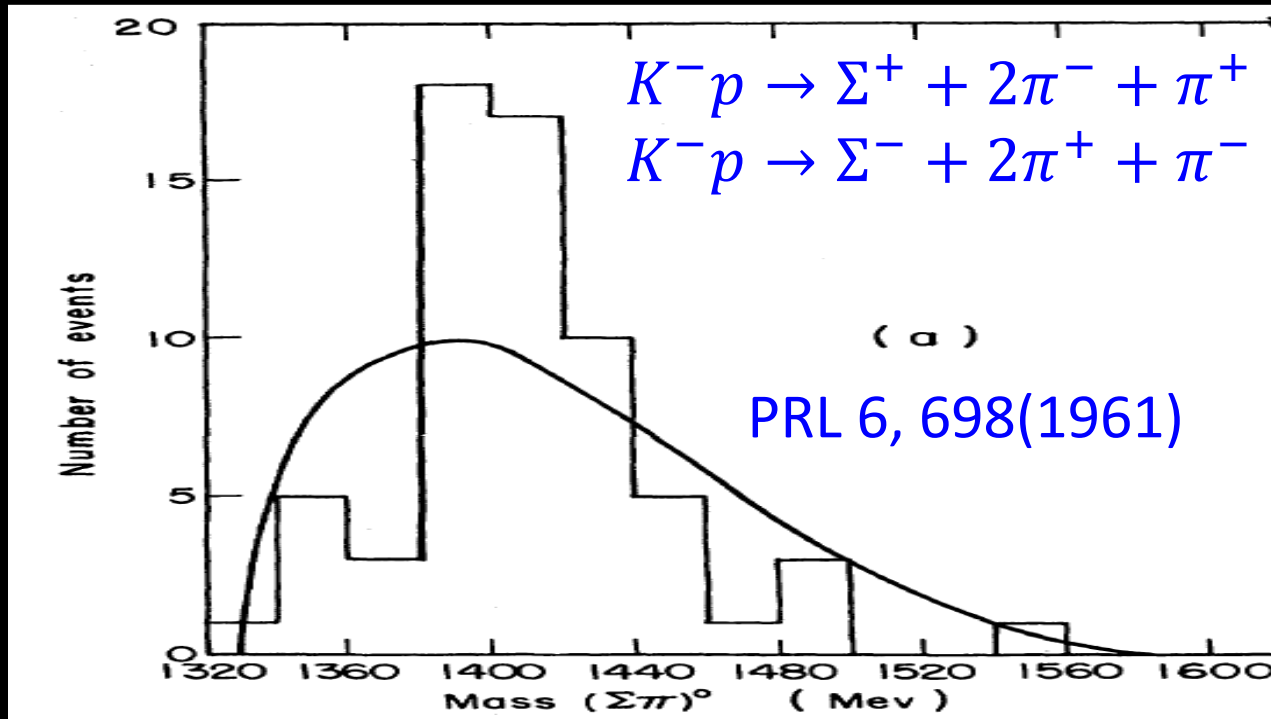
Anti-kaon nucleon scattering amplitude measured below the KN mass threshold

Hiroyuki Noumi^{*,#} for the J-PARC E31 collaboration

** RCNP, Osaka University*

Institute of Particle and Nuclear Studies, KEK

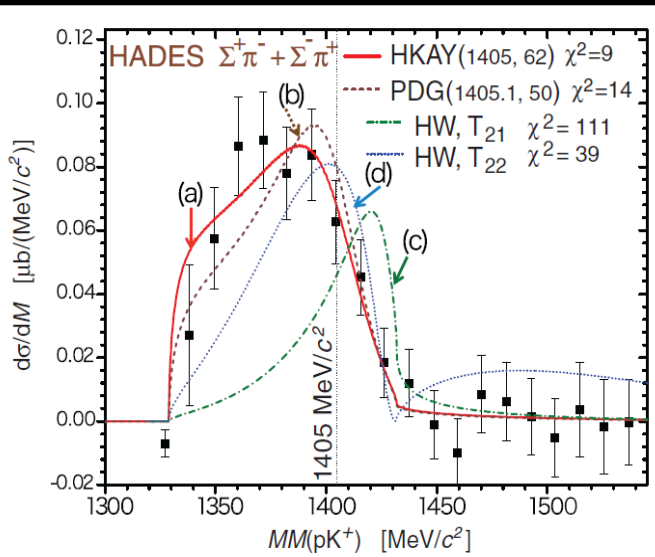
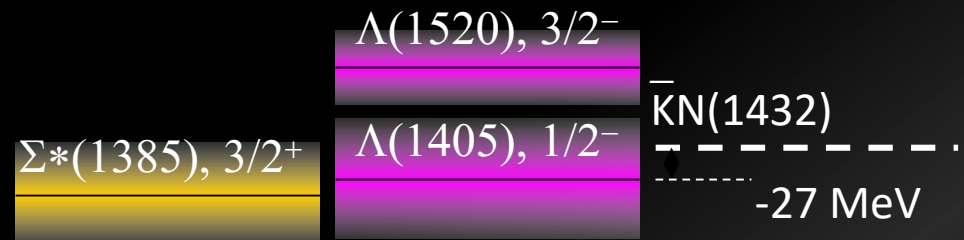
$\Lambda(1405)$ since 1961



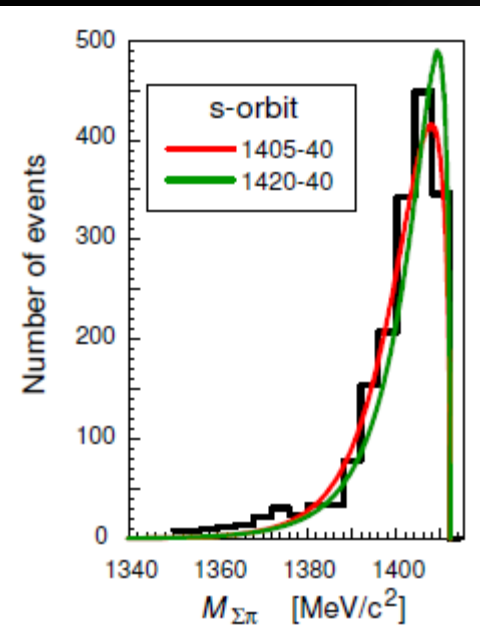
- Well-known lightest Hyperon Resonance w/ a negative parity, sitting just below the KbarN mass threshold

$\Lambda(1405) : 1405.1^{+1.3}_{-0.9} \text{ MeV}$ (PDG in 2020)

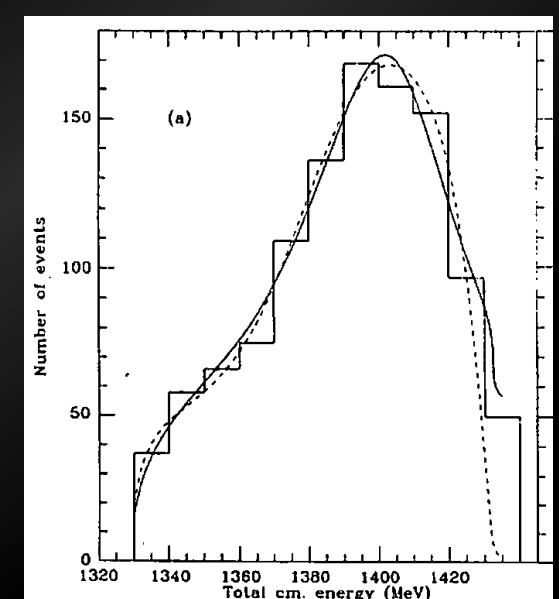
$J^P = \frac{1}{2}^-$, $I = 0$, $M_{\Lambda(1405)} < M_{K\bar{N}}$, lightest in neg. parity baryons



M. Hassanvand et al: $\pi\Sigma$ IM
Spec. of $pp \rightarrow K^+\pi\Sigma$



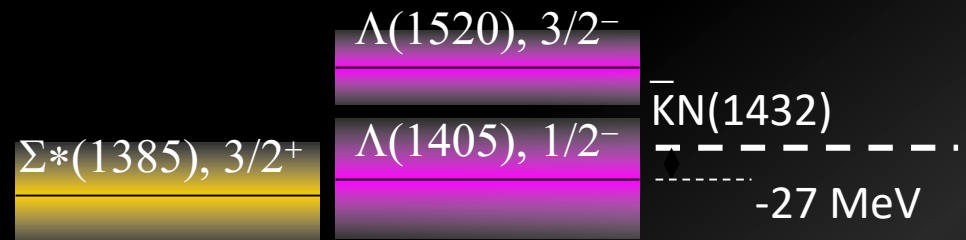
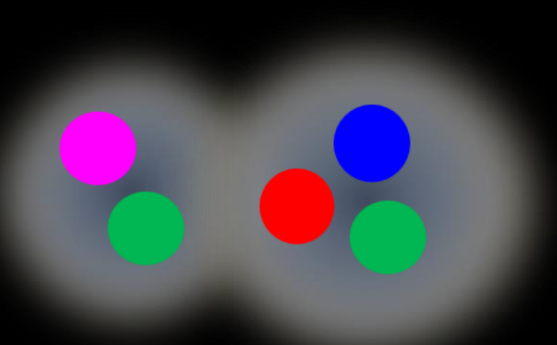
J. Esmaili et al: $\pi\Sigma$ IM Spec. of
Stopped K^- on ${}^4\text{He}$



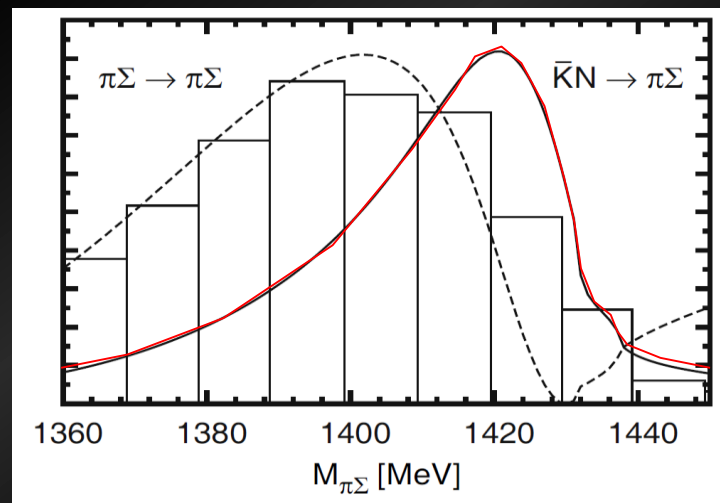
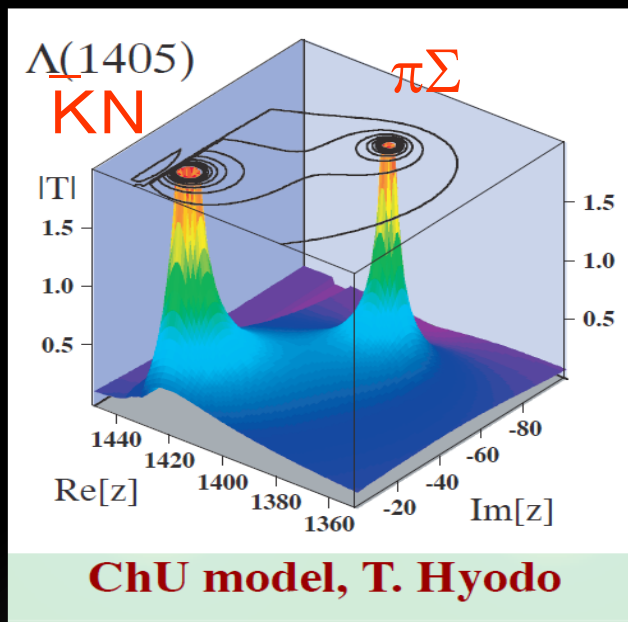
R.H. Dalitz et al: $\pi\Sigma$ IM Spec.
in $K^-p \rightarrow \pi\pi\Sigma$ w/ M-matrix

$\Lambda(1405)$: Double pole?

$J^P = \frac{1}{2}^-$, $I = 0$, $M_{\Lambda(1405)} < M_{K\bar{N}}$, lightest in neg. parity baryons



$$\frac{\Sigma(1192), 1/2^+}{\Lambda(1116), 1/2^+}$$



Chiral Unitary Model:
D. Jido et al., NPA725(03)181

Pole Structure of the Lambda(1405) Region

PDG Reviews: Ulf-G. Meissner and T. Hyodo (Nov. 2015)

$\Lambda(1405)$ POLE POSITION

REAL PART

VALUE (MeV)

• • • We do not use the following data for averages, fits, limits, etc. • • •

	DOCUMENT ID	TECN
1429 ^{+ 8} _{- 7}	¹ MAI	15 DPWA
1434 ^{+ 2} _{- 2}	² MAI	15 DPWA
1421 ^{+ 3} _{- 2}	GUO	13 DPWA
1424 ^{+ 7} _{- 23}	IKEDA	12 DPWA

¹Solution number 4.

²Solution number 2.

-2xIMAGINARY PART

VALUE (MeV)

• • • We do not use the following data for averages, fits, limits, etc. • • •

	DOCUMENT ID	TECN
24 ^{+ 4} _{- 6}	¹ MAI	15 DPWA
20 ^{+ 4} _{- 2}	² MAI	15 DPWA
38 ^{+ 16} _{- 10}	GUO	13 DPWA
52 ^{+ 6} _{- 28}	IKEDA	12 DPWA

¹Solution number 4.

²Solution number 2.

$\Lambda(1380)$ POLE POSITION

REAL PART

VALUE (MeV)

• • • We do not use the following data for averages, fits, limits, etc. • • •

	DOCUMENT ID	TECN
1325 \pm 15	¹ MAI	15 DPWA
1330 ^{+ 4} _{- 5}	² MAI	15 DPWA
1388 \pm 9	GUO	13 DPWA
1381 ^{+ 18} _{- 6}	IKEDA	12 DPWA

¹Solution number 4.

²Solution number 2.

-2xIMAGINARY PART

VALUE (MeV)

• • • We do not use the following data for averages, fits, limits, etc. • • •

	DOCUMENT ID	TECN
180 ^{+ 24} _{- 36}	¹ MAI	15 DPWA
112 ^{+ 34} _{- 22}	² MAI	15 DPWA
228 ^{+ 48} _{- 50}	GUO	13 DPWA
162 ^{+ 38} _{- 16}	IKEDA	12 DPWA

¹Solution number 4.

²Solution number 2.

$\Lambda(1405) : 1405.1^{+1.3}_{-1.0}$ MeV (Part. Listing in '20)

$J^P = \frac{1}{2}^-$, $I = 0$, $M_{\Lambda(1405)} < M_{K\bar{N}}$, lightest in neg. parity baryons

M. Hassanvand et al: $\pi\Sigma$ IM
Spec. of $p\bar{p} \rightarrow K^+\pi\Sigma$

J. Esmaili et al: $\pi\Sigma$ IM Spec. of
Stopped K^- on ${}^4\text{He}$

R.H. Dalitz et al: $\pi\Sigma$ IM Spec.
in $K-p \rightarrow \pi\pi\Sigma$ w/ M-matrix

TABLE II. Pole positions of the T -matrix in the $\bar{K}N$ and $\pi\Sigma$ single-channel scatterings and the $\bar{K}N$ - $\pi\Sigma$ coupled channels without on-shell factorization, A and B , and with on-shell factorization, C .

	Single channel		Coupled channels	
	$\bar{K}N$	$\pi\Sigma$	$\bar{K}N$ - $\pi\Sigma$	
A	1432 MeV	1388-179 <i>i</i> MeV	1434-7 <i>i</i> MeV	1418-160 <i>i</i> MeV
B	1425 MeV	1382-169 <i>i</i> MeV	1419-19 <i>i</i> MeV	1424-146 <i>i</i> MeV
C	1427 MeV	1388-96 <i>i</i> MeV	1432-17 <i>i</i> MeV	1398-73 <i>i</i> MeV

REAL PART
VALUE (MeV)

• • • We do not use

1429 $^{+8}_{-7}$

1434 ± 2

1421 $^{+3}_{-2}$

1424 $^{+7}_{-23}$

¹Solution number
²Solution number

-2xIMAGINARY

VALUE (MeV)

• • • We do not use the following data for averages, fits, limits, etc. • • •

24 $^{+4}_{-6}$

¹ MAI 15 DPWA

VALUE (MeV)

• • • We do not use the following data for averages, fits, limits, etc. • • •

180 $^{+24}_{-36}$ 1 MAI 15 DPWA

20 $^{+4}_{-2}$

² MAI 15 DPWA

112 $^{+34}_{-22}$ 2 MAI 15 DPWA

38 $^{+16}_{-10}$

GUO 13 DPWA

228 $^{+48}_{-50}$ GUO 13 DPWA

52 $^{+6}_{-28}$

IKEDA 12 DPWA

162 $^{+38}_{-16}$ IKEDA 12 DPWA

¹Solution number 4.

²Solution number 2.

¹Solution number 4.

²Solution number 2.

$\Lambda(1405) : 1405.1^{+1.3}_{-1.0}$ MeV (Part. Listing in '20)

$J^P = \frac{1}{2}^-$, $I = 0$, $M_{\Lambda(1405)} < M_{K\bar{N}}$, lightest in neg. parity baryons

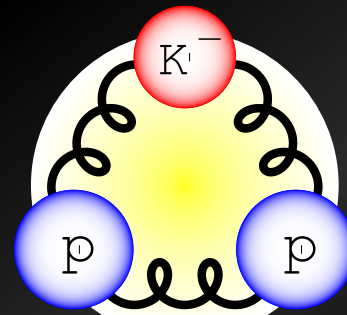
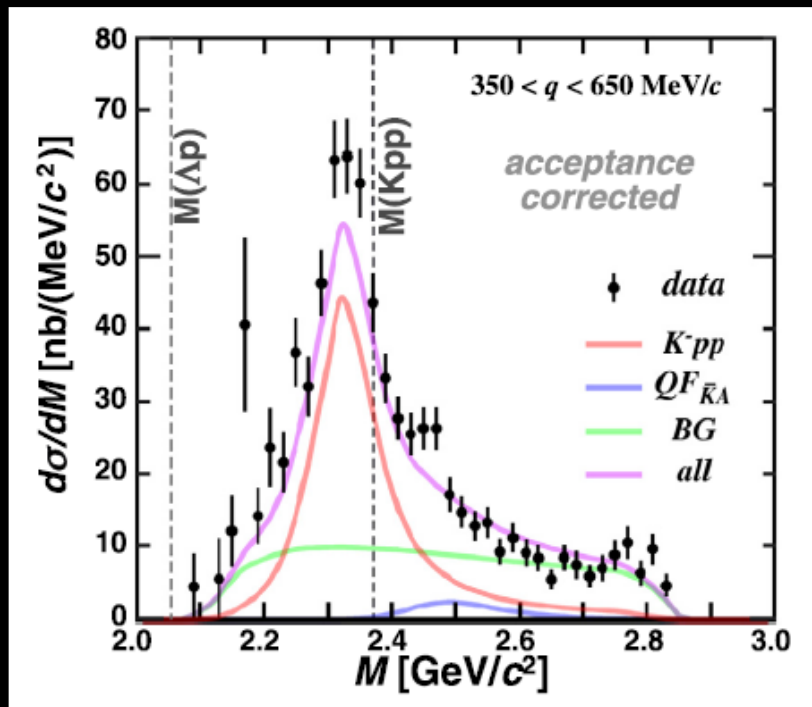
M. Hassanvand et al: $\pi\Sigma$ IM
Spec. of $p p \rightarrow K^+\pi\Sigma$

J. Esmaili et al: $\pi\Sigma$ IM Spec. of
Stopped K^- on ${}^4\text{He}$

R.H. Dalitz et al: $\pi\Sigma$ IM Spec.
in $K-p \rightarrow \pi\pi\Sigma$ w/ M-matrix

Questions on $\Lambda(1405)$

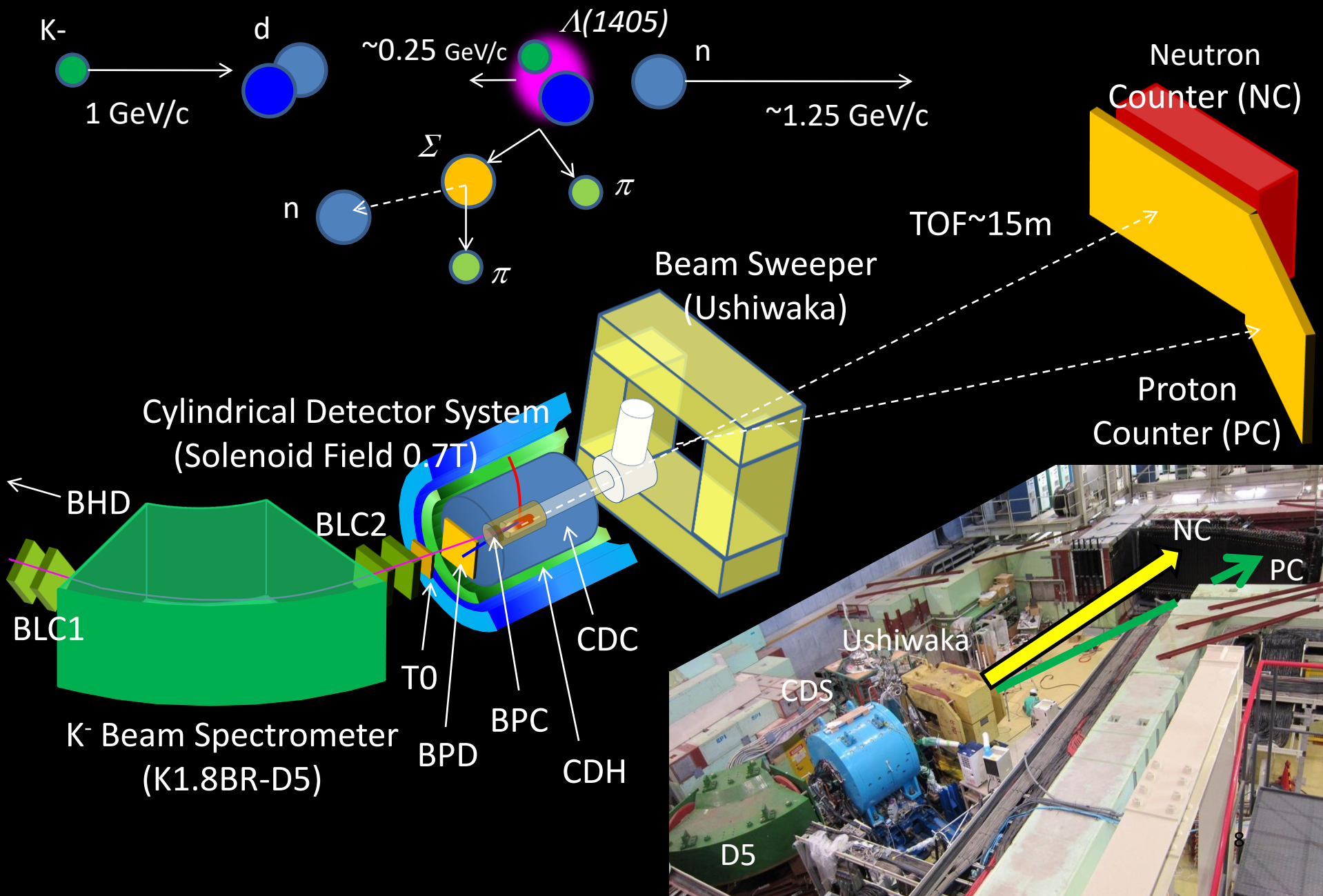
- $K^{\bar{N}}$ int. and its pole position are still unclear.
 - Basic information on Kaonic Nuclei



E15 Collaboration
Physics Letters B 789 (2019) 620–625
Phys. Rev. C102, 044002 (2020).

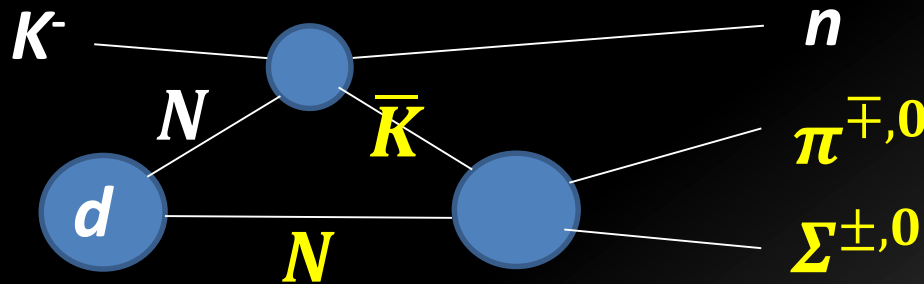
Important to study Low Energy $K^{\bar{N}}$ scattering

Experimental Setup for E31



$K^{\bar{b}ar}N$ scattering below the $K^{\bar{b}ar}N$ thres. (J-PARC E31)

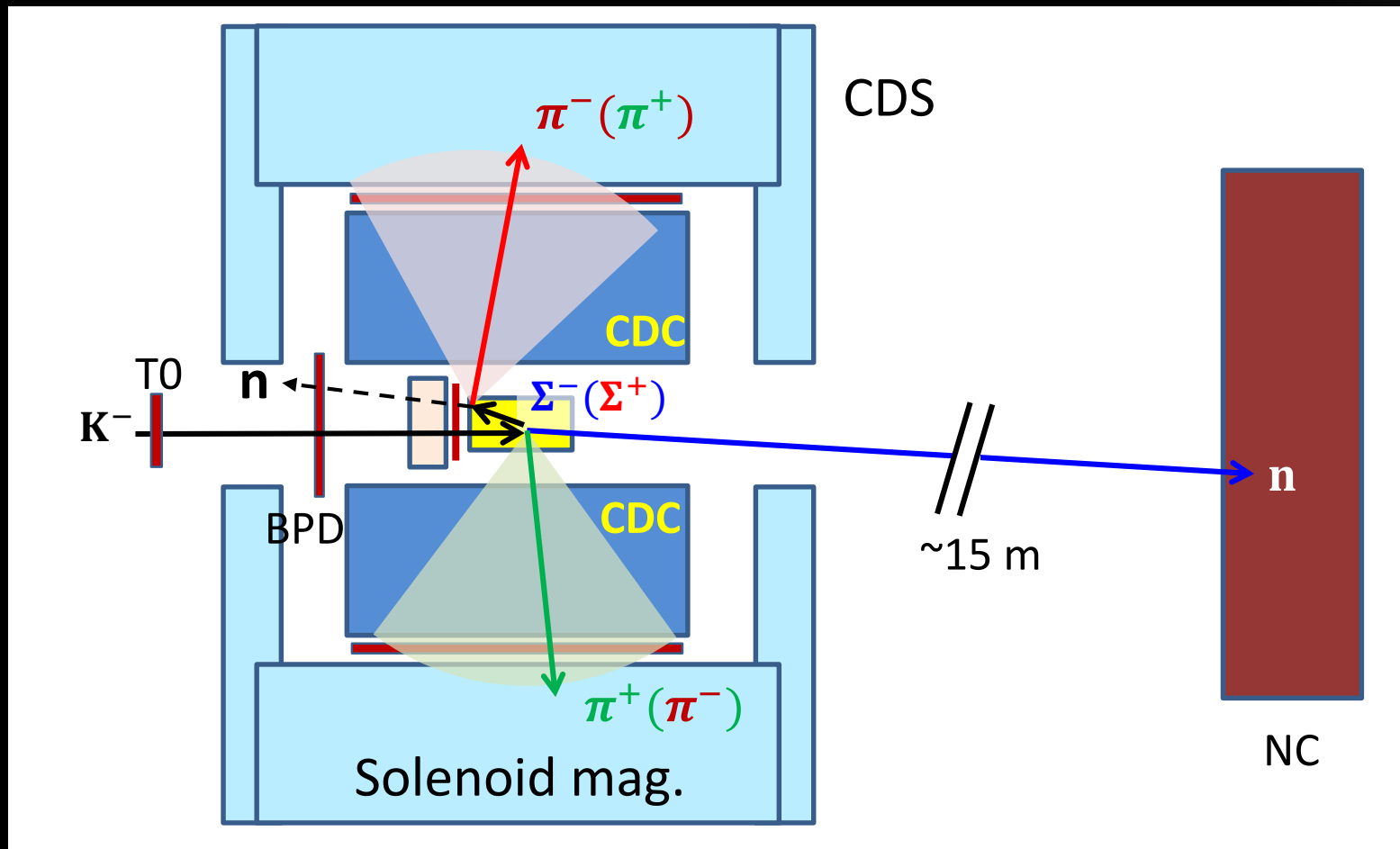
- measuring an *S-wave* $\bar{K}N \rightarrow \pi\Sigma$ scattering below the $\bar{K}N$ threshold in the $d(K^-, n)\pi\Sigma$ reactions at a forward angle of n .



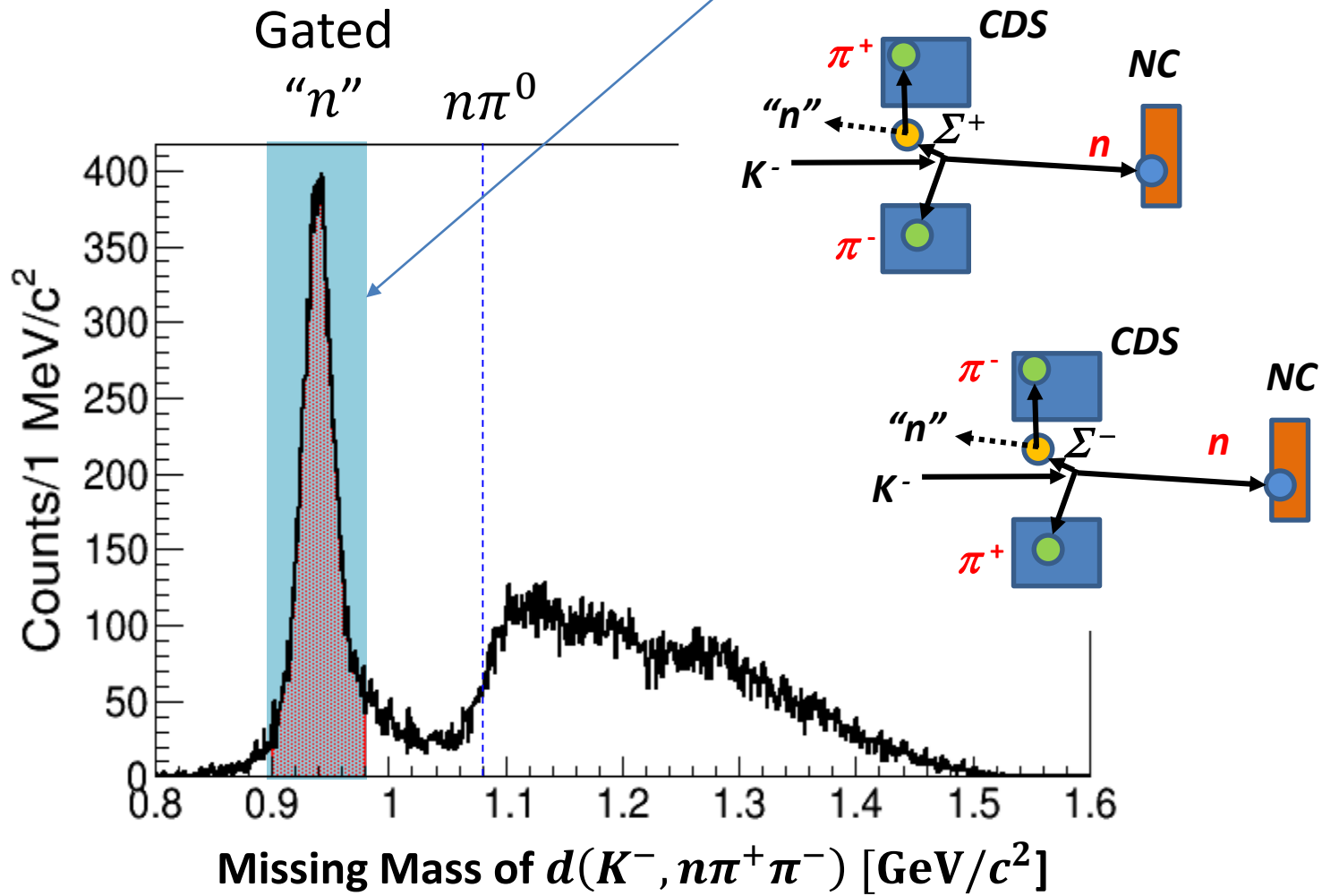
- ID's all the final states to decompose the $l=0$ and 1 ampl's.

$\pi^\pm\Sigma^\mp$	$l=0, 1$	$\Lambda(1405)$ ($l=0$, S wave), non-resonant [$l=0/1$] $(\Sigma(1385))$ ($l=1$, P wave) to be suppressed)
$\pi^-\Sigma^0$ [$\pi^-\Lambda$]	$l=1$	non-resonant ($\Sigma(1385)$ to be suppressed) $d(K^-, p)\pi^-\Sigma^0$ [$\pi^-\Lambda$]
$\pi^0\Sigma^0$	$l=0$	$\Lambda(1405)$ ($l=0$, S wave), non-resonant

Event topology of $d(K^-, n)X_{\pi^\pm\Sigma^\mp}$



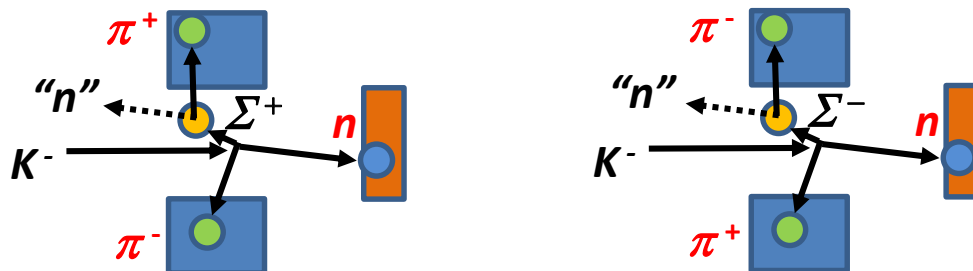
$d(K^-, n\pi^+\pi^-) n_{missing}$



$d(K^-, n\pi^+\pi^-)$ " n " samples contain...

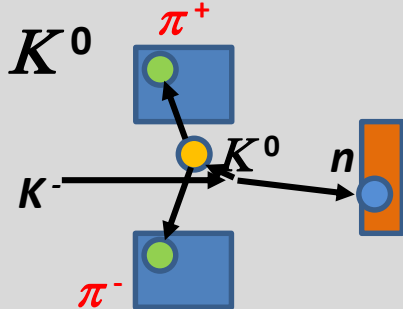
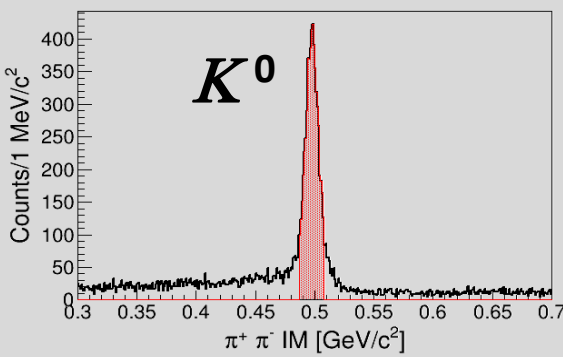
Signal Events

$$d(K^-, n) X_{\pi^\pm \Sigma^\mp}$$

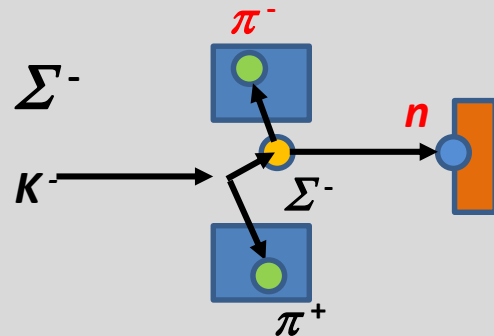
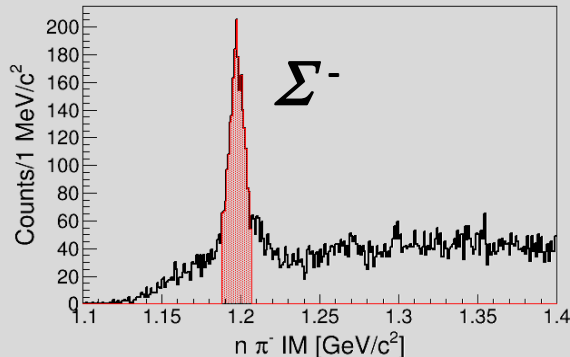


Major Background Events

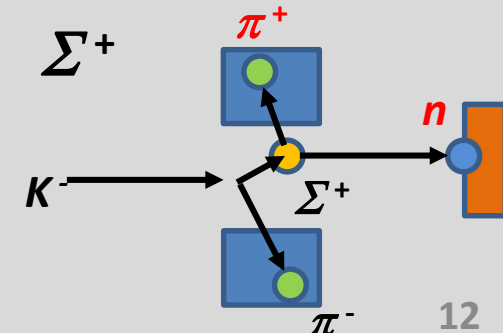
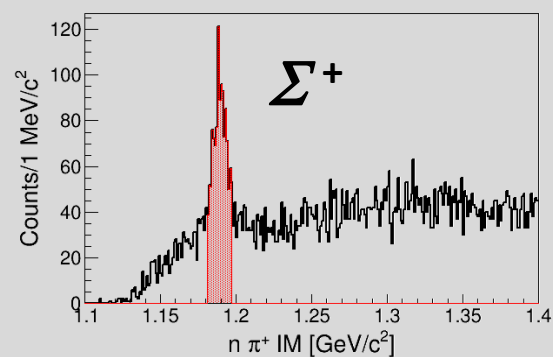
CDS $\pi^+ \pi^-$ IM



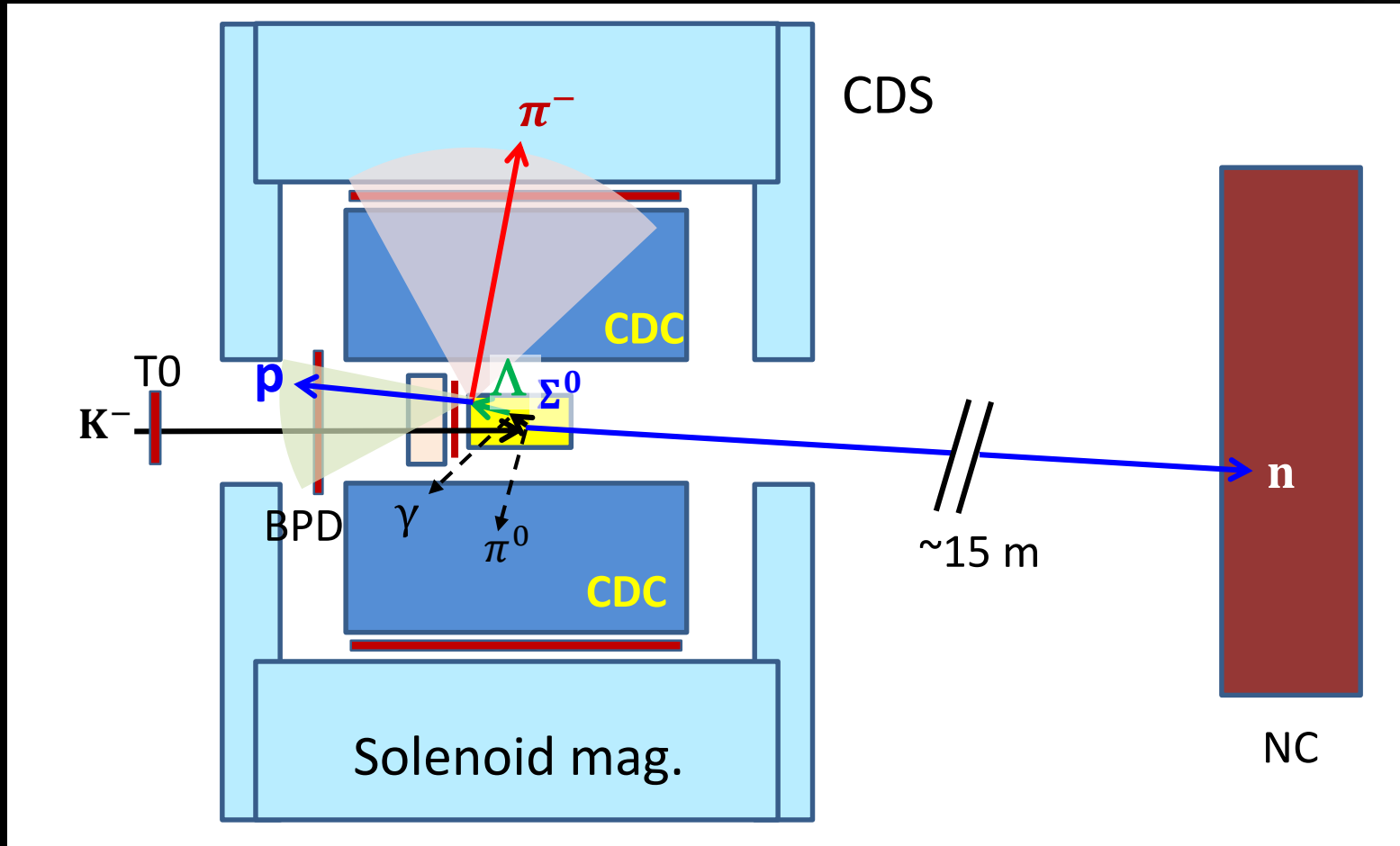
$n \pi^-$ w/ π^+



$n \pi^-$ w/ π^+

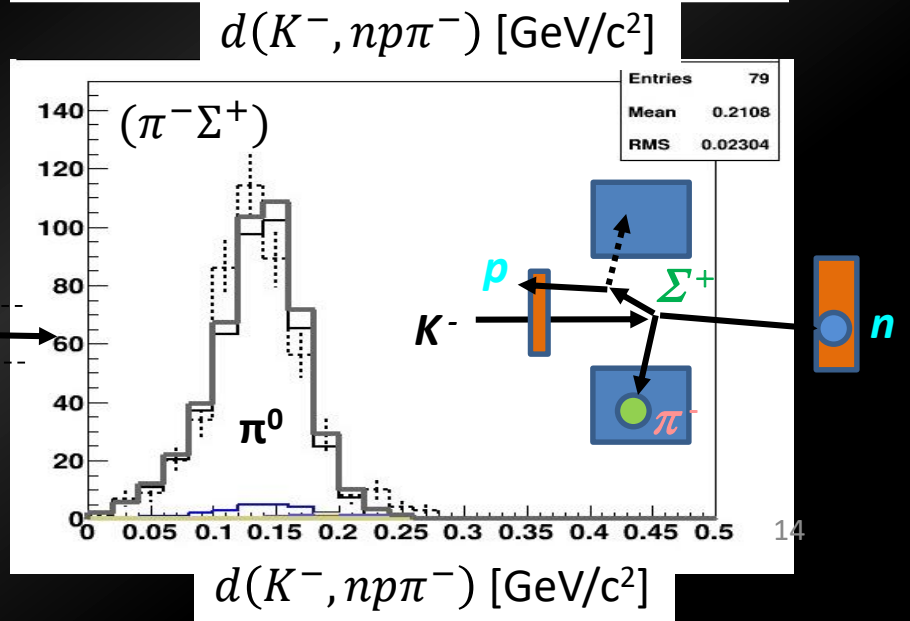
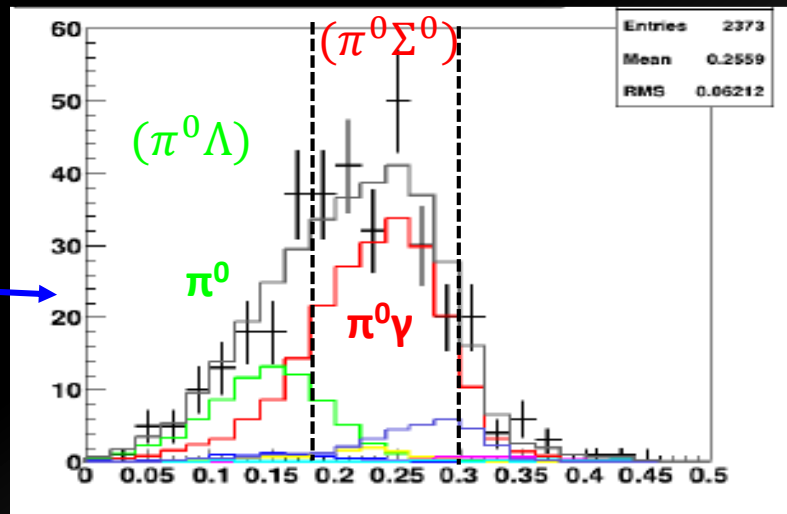
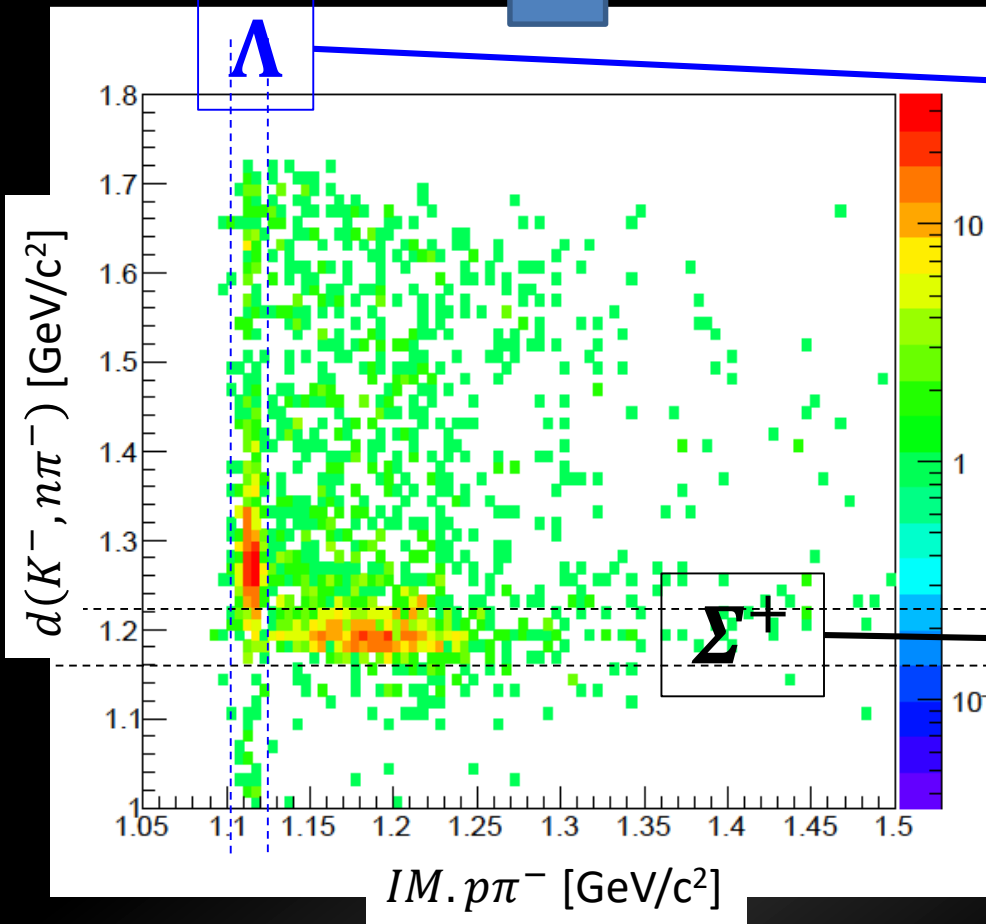
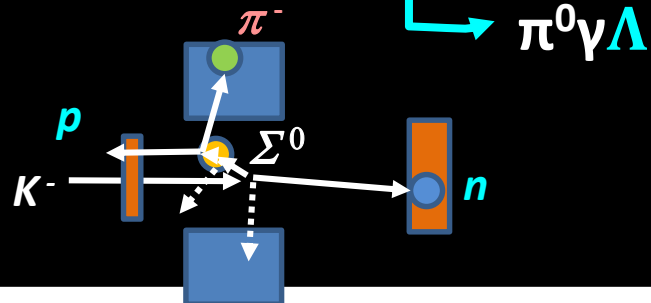


Event topology of $d(K^-, n)X_{\pi^0 \Sigma^0}$

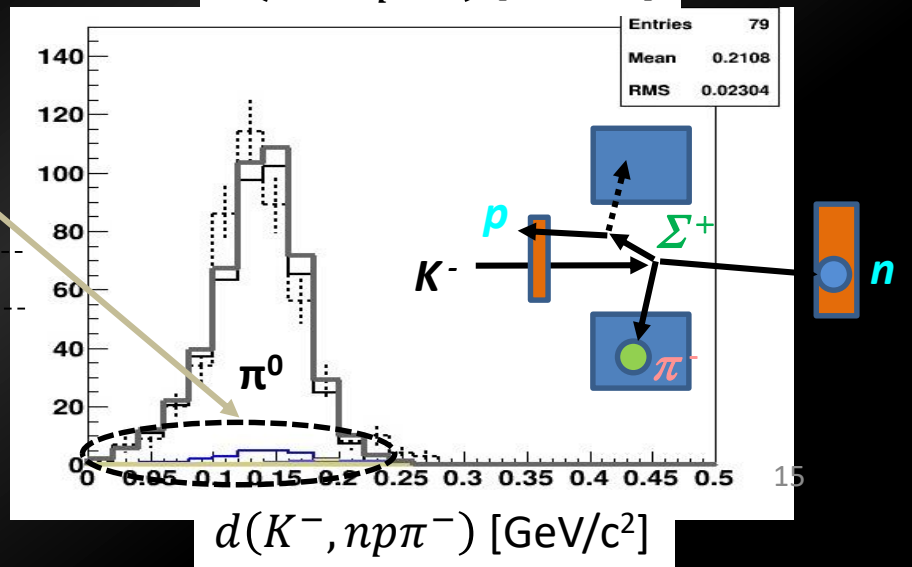
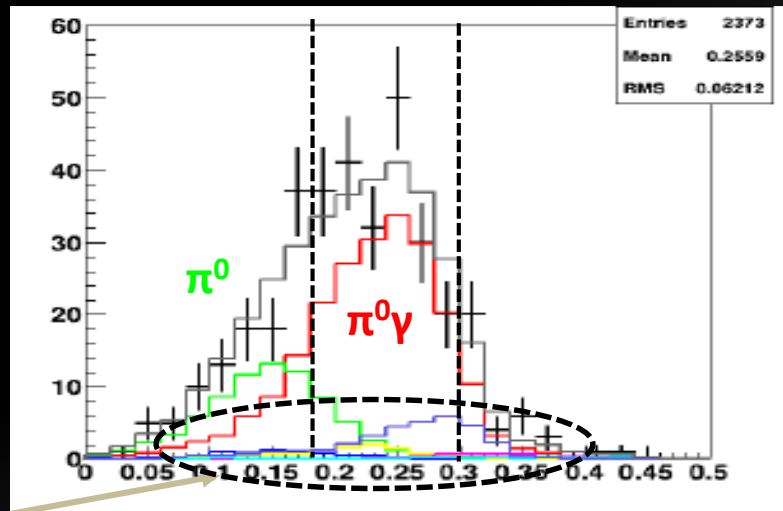
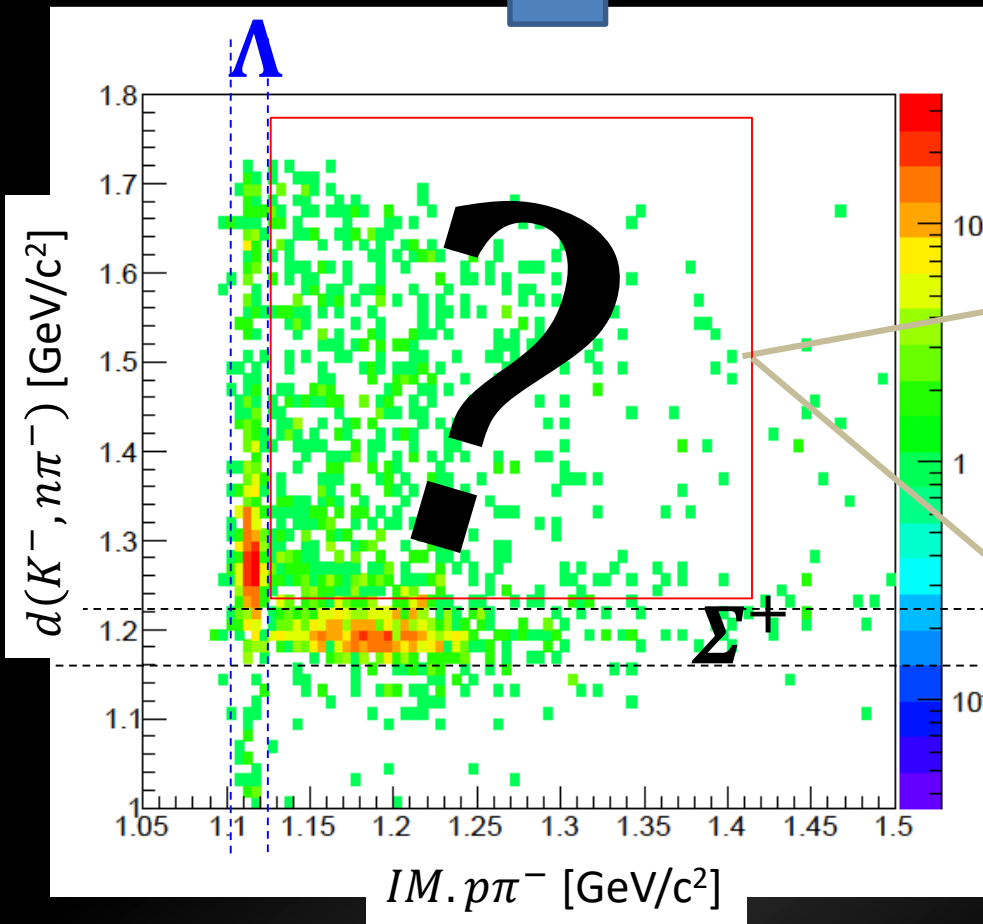
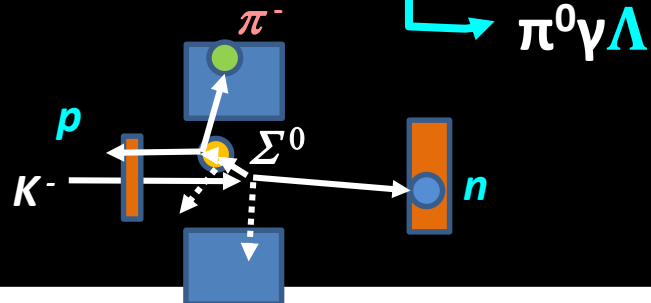


BG Process: $d(K^-, n)X_{\pi^0 \Lambda}$, $d(K^-, n)X_{\pi^0 \pi^0 \Lambda}$,
 $d(K^-, n)X_{\pi^- \Sigma^+}$, $d(K^-, \Sigma^- p)X$

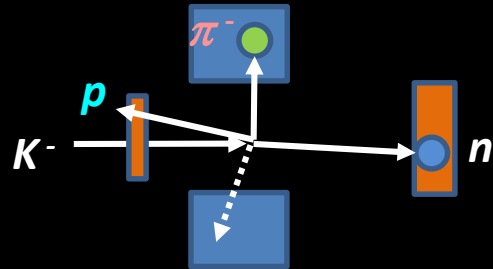
$d(K^-, n) \frac{\pi^0 \Sigma^0}{\pi^0 \gamma \Lambda}$ vs $d(K^-, n) \frac{\pi^- \Sigma^+}{\pi^- p \pi^0}$



$d(K^-, n) \frac{\pi^0 \Sigma^0}{\pi^0 \gamma \Lambda}$ vs $d(K^-, n) \frac{\pi^- \Sigma^+}{\pi^- p \pi^0}$



$d(K^-, n)\pi^0\Sigma^0$ vs $d(K^-, n)\pi^-\Sigma^+$



Other BG processes

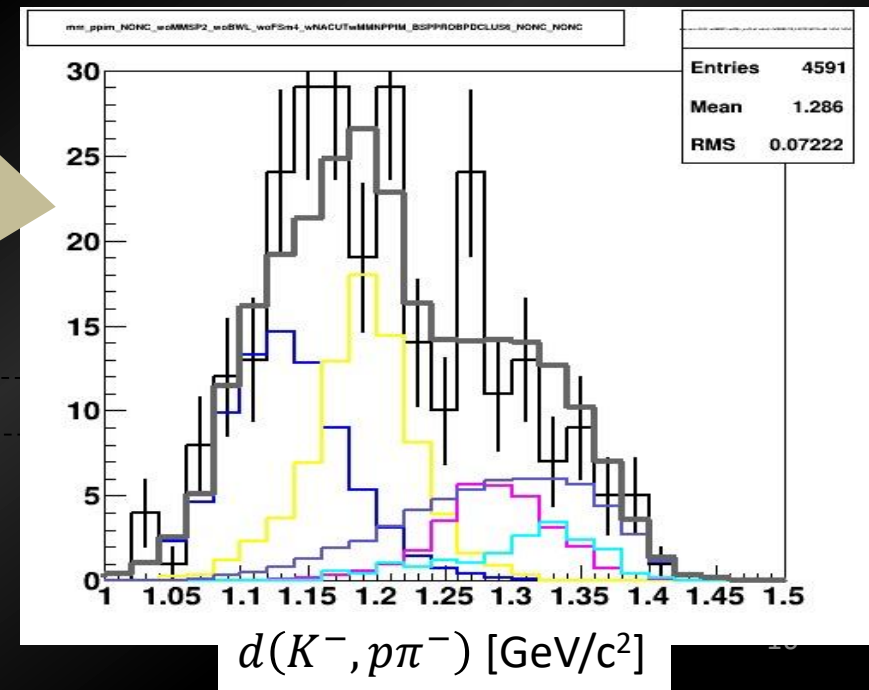
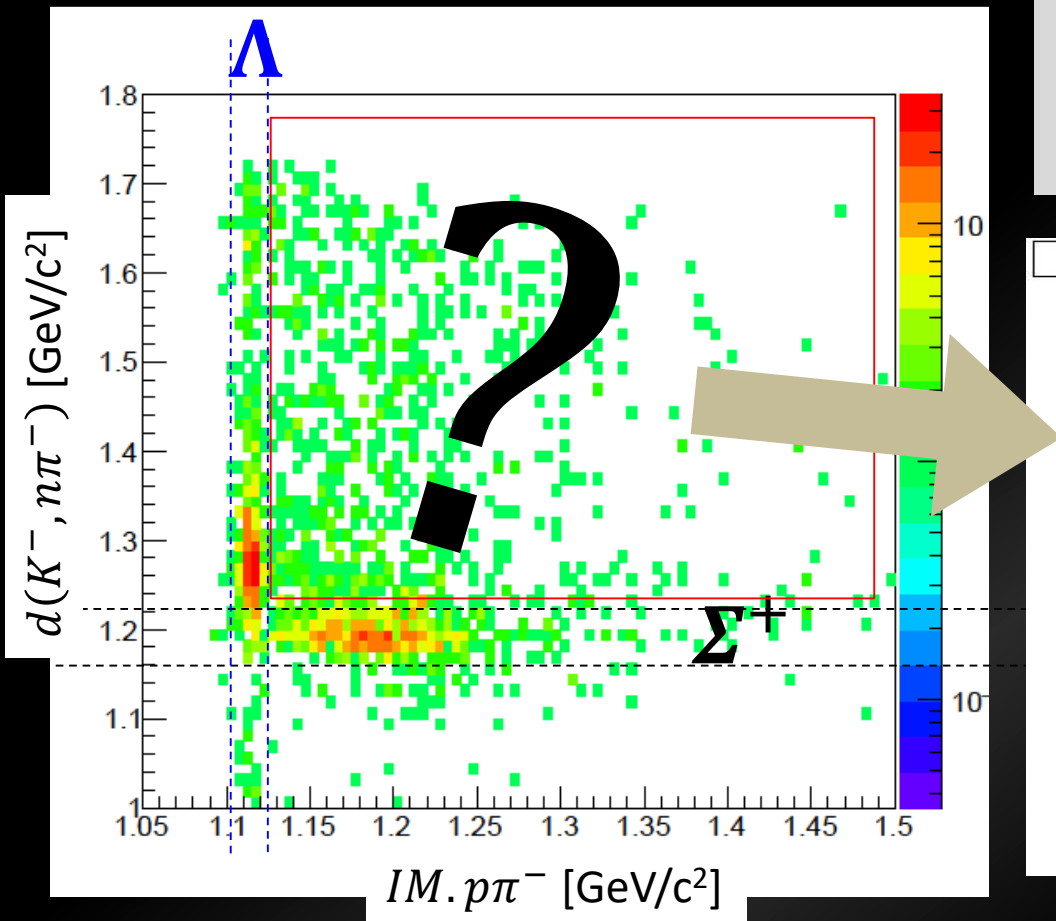
$$d(K^-, p\pi^-)X$$

$$X = \underline{\Lambda, \Sigma^0, \Lambda\pi^0, \Sigma^0\pi^0}$$

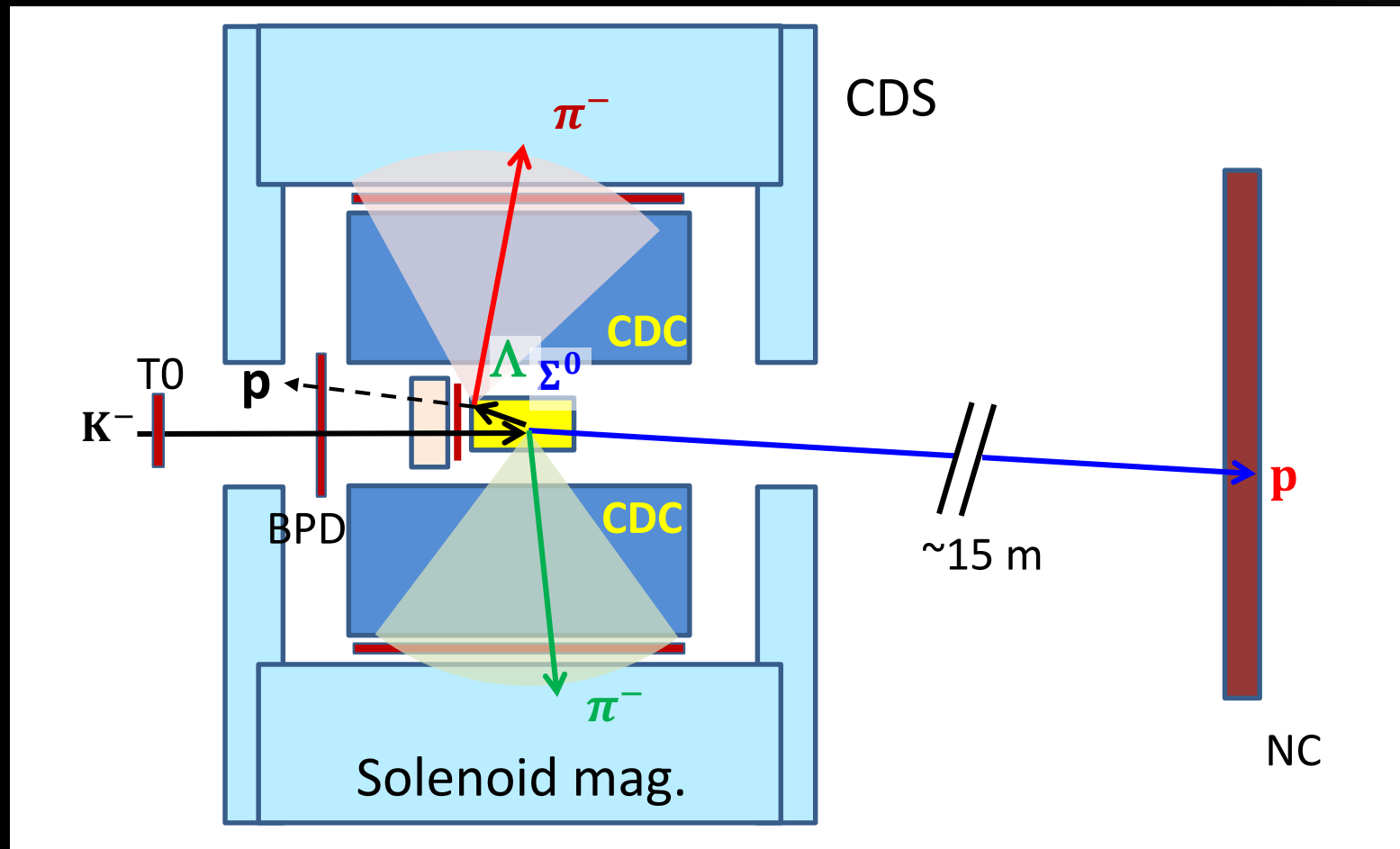
$\downarrow n$ (to NC)

$$d(K^-, n)K^-, d'(stopped K^-, N)X$$

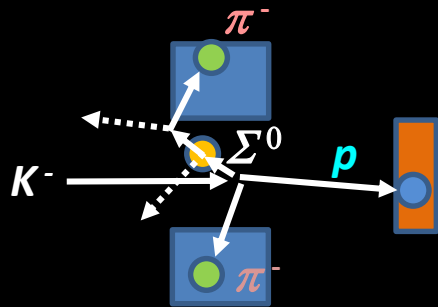
$$X = \Lambda\pi^0, \Lambda\pi^-, \Sigma^0\pi^0, \Sigma^0\pi^-, \Sigma^+\pi^-$$



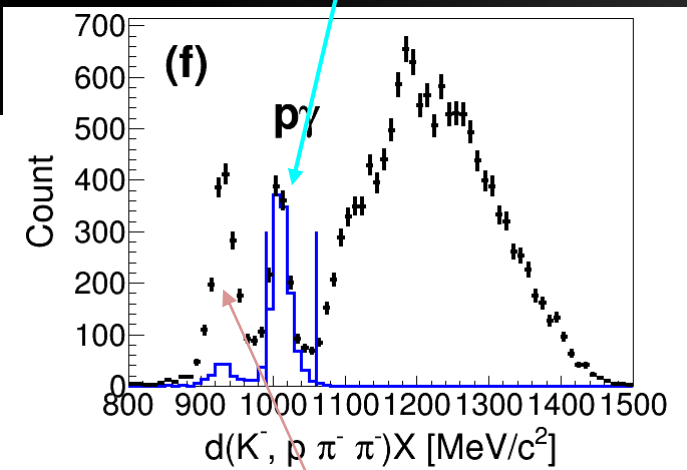
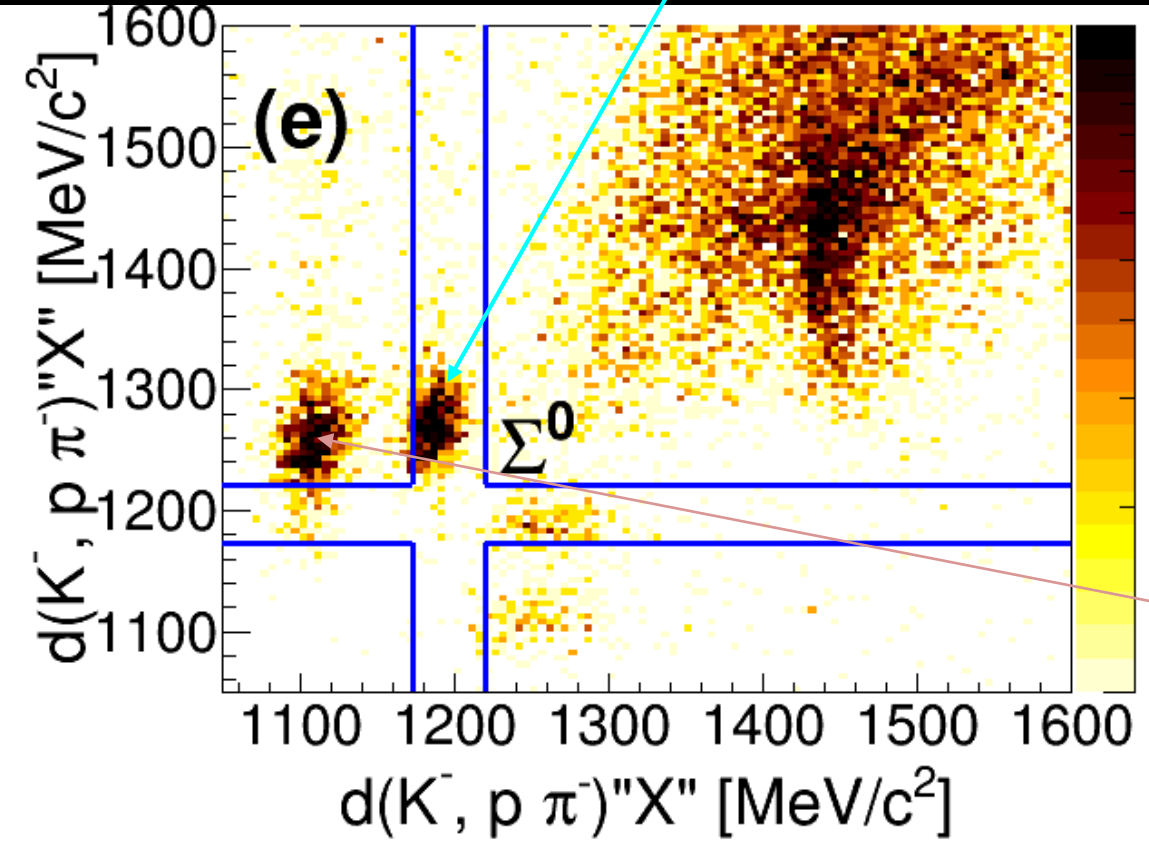
Event topology of $d(K^-, p)X_{\pi^-\Sigma^0}$



$d(K^-, p)X_{\pi^-\Sigma^0}$ Mode ($I = 1$)



From $d(K^-, p\pi^-\pi^-)$ " $p\gamma$ " sample

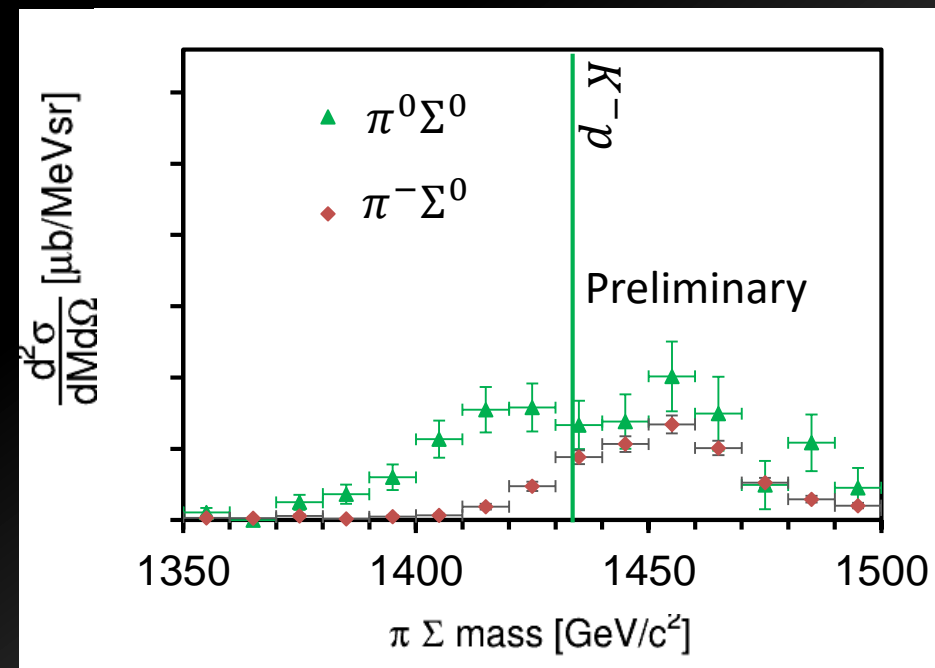
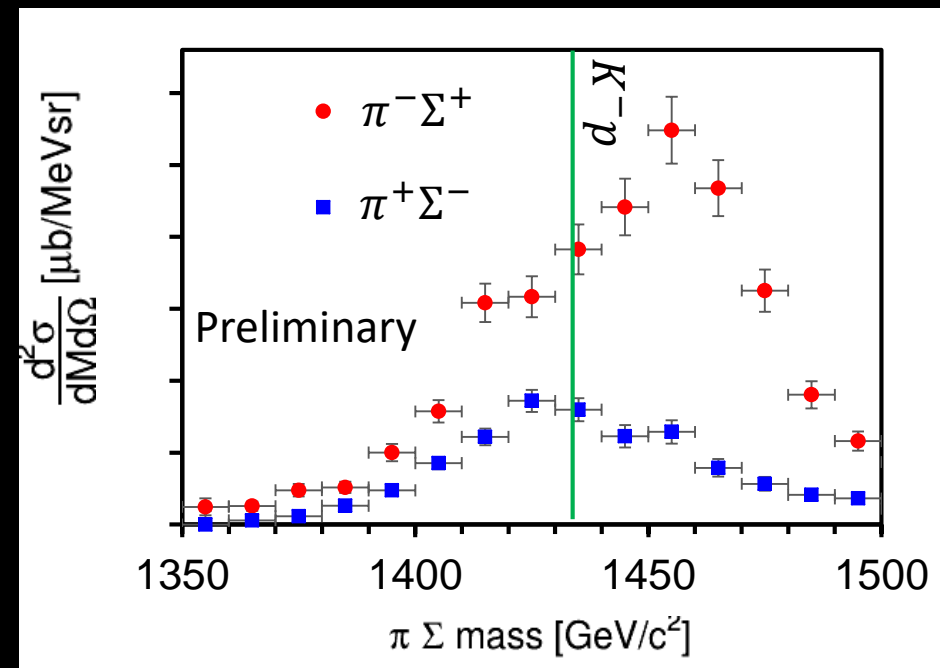


$d(K^-, p\pi^-\pi^-)$ " p "

$d(K^-, p)X_{\pi^-}$

$\pi^+\Sigma^-/\pi^-\Sigma^+$
 $(I = 0, 1)$

$\pi^0\Sigma^0(I = 0)$
 $\pi^-\Sigma^0(I = 1)$

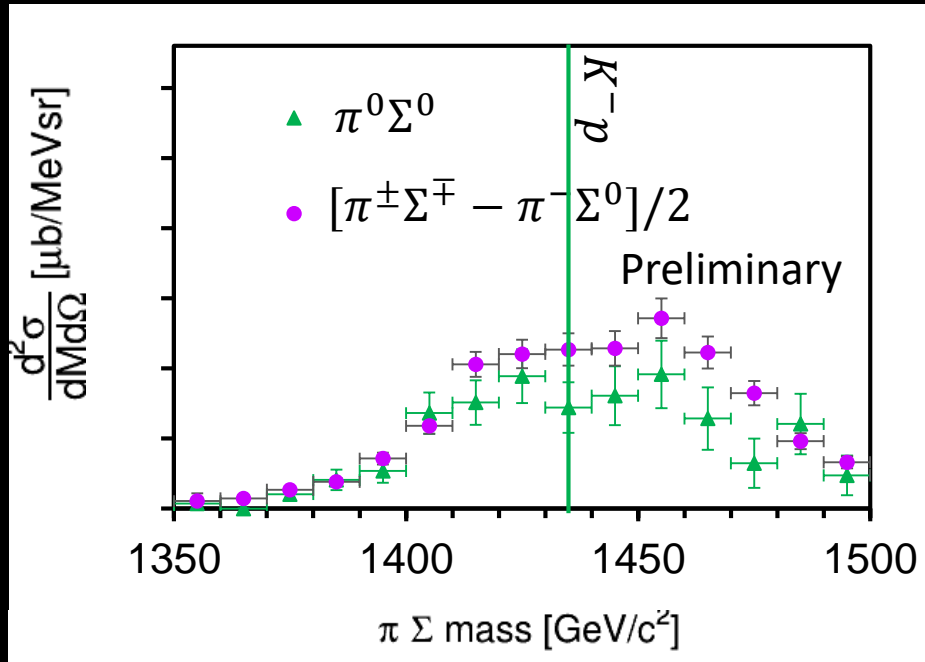


$$\frac{d\sigma}{d\Omega}(\pi^-\Sigma^+/\pi^+\Sigma^-) \propto \frac{1}{3}|f_{I=0}|^2 + \frac{1}{2}|f_{I=1}|^2 \pm \frac{\sqrt{6}}{3}\text{Re}(f_{I=0}f_{I=1}^*)$$

$$\frac{d\sigma}{d\Omega}(\pi^0\Sigma^0) \propto \frac{1}{3}|f_{I=0}|^2$$

$$\frac{d\sigma}{d\Omega}(\pi^-\Sigma^0) \propto |f_{I=1}|^2$$

$[\pi^\pm \Sigma^\mp - \pi^- \Sigma^0]/2$ vs $\pi^0 \Sigma^0 (I = 0)$

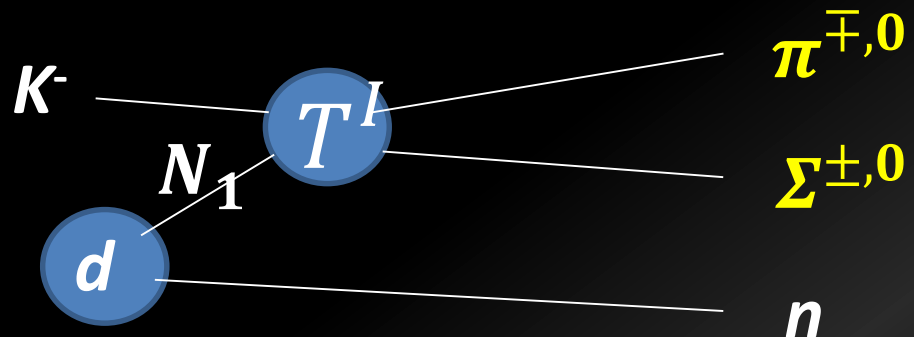


$$\frac{d\sigma}{d\Omega}([\pi^\pm \Sigma^\mp - \pi^- \Sigma^0]/2) \propto \frac{1}{3} |f_{I=0}|^2$$

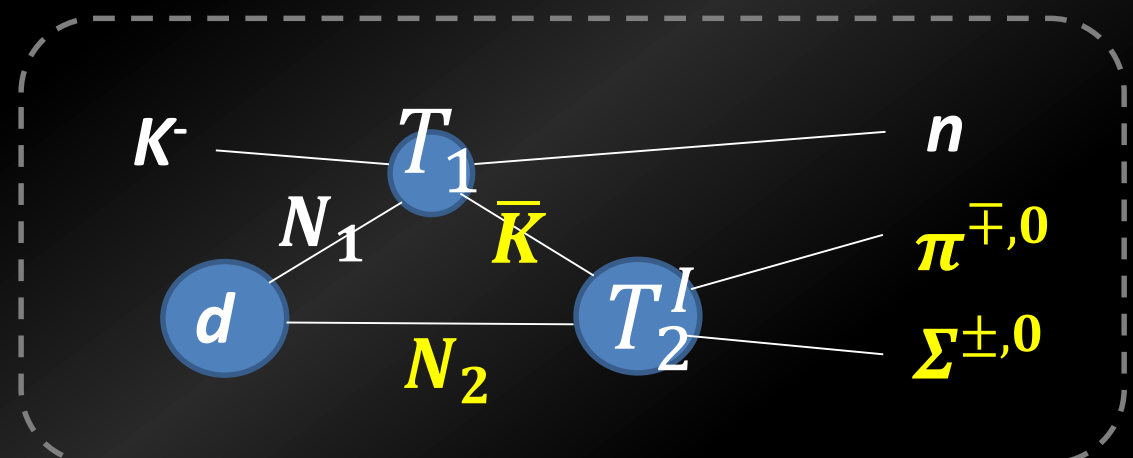
$$\frac{d\sigma}{d\Omega}(\pi^0 \Sigma^0) \propto \frac{1}{3} |f_{I=0}|^2$$

Description of the reaction

- 1-step process

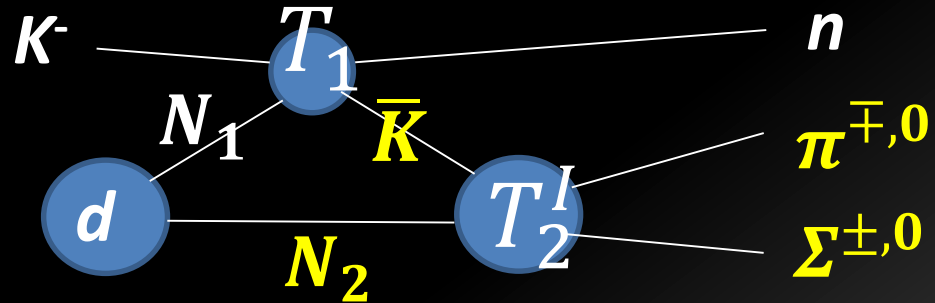


- 2-step process



Extracting Scattering Amplitude

- 2-step process



$$\begin{aligned} \frac{d\sigma}{dM_{\pi\Sigma}} \Big|_{\theta_n=0} &\sim | \langle n\pi\Sigma | T_2^I(\bar{K}N \rightarrow \pi\Sigma) G_0 T_1(K^-N \rightarrow \bar{K}N) | K^- \Phi_d \rangle |^2 \\ &\sim |T_2^I(\bar{K}N \rightarrow \pi\Sigma)|^2 F_{\text{res}}(M_{\pi\Sigma}) \end{aligned}$$

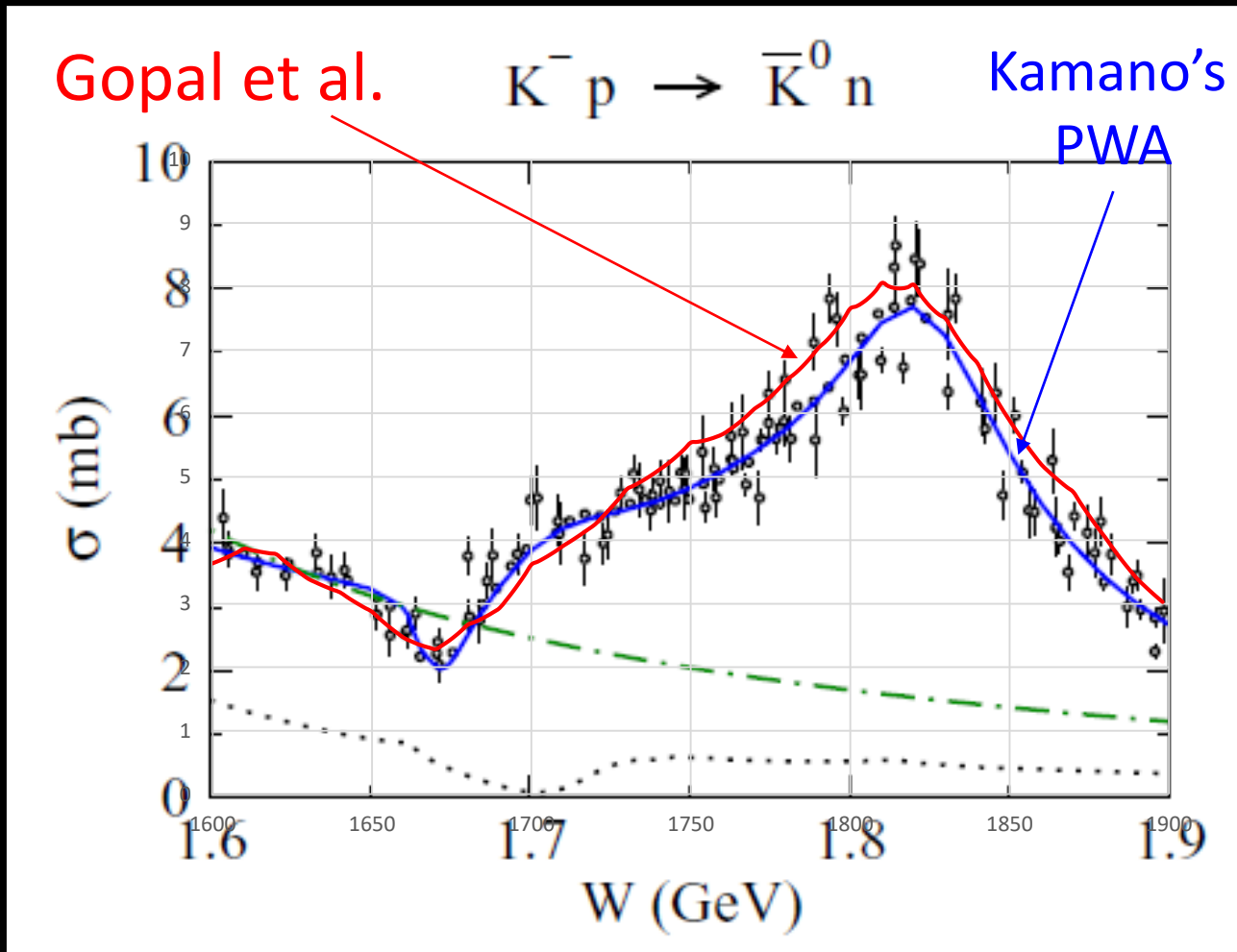
Factorization Approximation

$$F_{\text{res}}(M_{\pi\Sigma}) \sim \left| \int_0^\infty dq_{N_2}^3 T_1 \frac{1}{E_{\bar{K}} - E_{\bar{K}}(q_{\bar{K}}) + i\epsilon} \Phi_d(q_{N_2}) \right|^2, q_{\bar{K}} + q_{N_2} = q_{\pi\Sigma}$$

E31: Response Function, $F_{\text{res}}(M_{\pi\Sigma})$

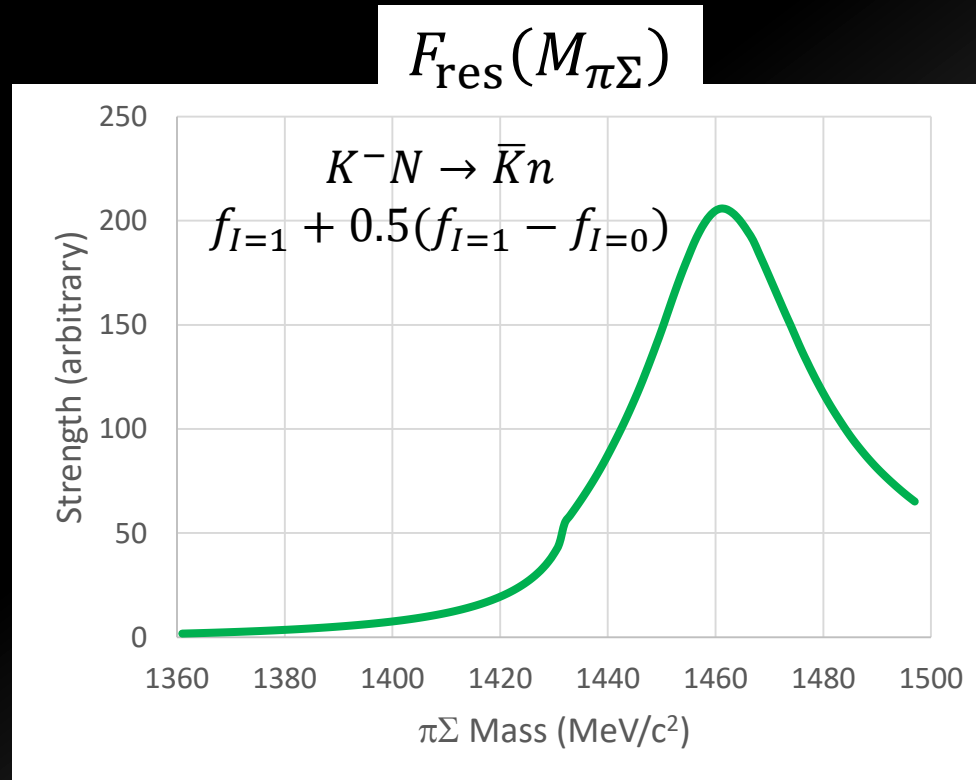
- $F_{\text{res}}(M_{\pi\Sigma}) = \left| \int G_0(q_2, q_1) T_1 \Phi_d(q_2) d^3 q_2 \right|^2$
 - $G_0(q_2, q_1) = \frac{1}{q_0^2 - q'^2 + i\varepsilon} f(q_0, q') \frac{\left(\sqrt{P_{\pi\Sigma}^2 + M_{\pi\Sigma}^2} + \sqrt{P_{\pi\Sigma}^2 + W(q')^2} \right)}{M_{\pi\Sigma} + W(q')}$,
 $f(q_0, q')^{-1} = [E_1(q_0) + E_1(q')]^{-1} + [E_2(q_0) + E_2(q')]^{-1}$
K. Miyagawa and J. Haidenbauer, PRC85, 065201(2012)
 - $T_1: K^- n \rightarrow K^- n$ ($I = 1$), $K^- p \rightarrow \bar{K}^0 n$ ($I = 0, 1$) amplitude,
Gopal et al., NPB119, 362(1977)
 - $T_1(K^- n \rightarrow K^- n) = f(I = 1)$
 - $T_1(K^- p \rightarrow \bar{K}^0 n) = [f(I = 1) - f(I = 0)]/2$
- Off-shell treatment : See eq.(17) in PRC94, 065205
- $\Phi_d(q_2)$: deuteron wave function, **PRC63, 024001(2001)**

Elementary Cross Section for T_1



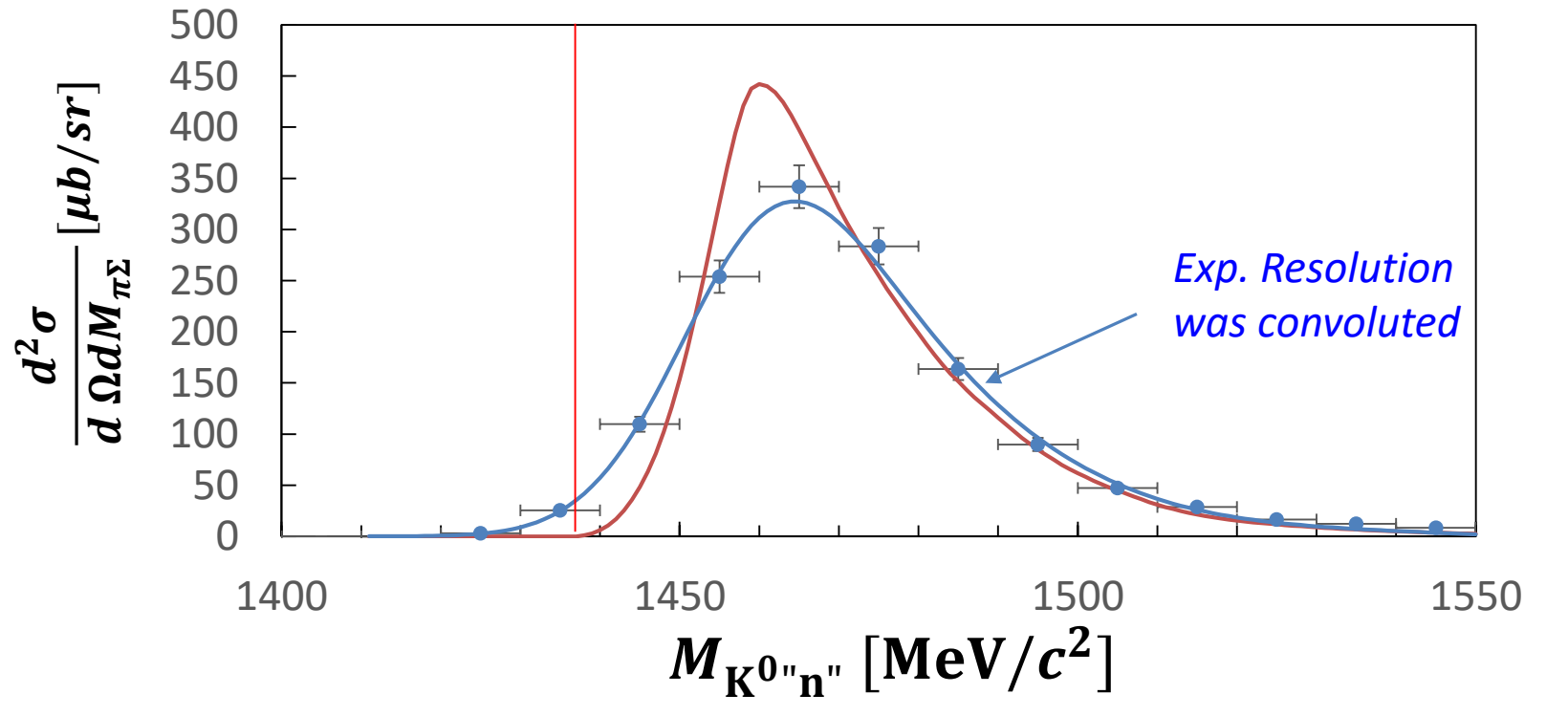
E31: Response Function, $F_{\text{res}}(M_{\pi\Sigma})$

$$F_{\text{res}}(M_{\pi\Sigma}) \sim p_\pi^{cm} p_n^2 / |(E_{K^-} + m_d)\beta_n - p_{K^-} \cos \theta| \times \\ \int d\Omega_\pi^{cm} E_\pi E_\Sigma \left| \int q_2 T_1(p_{K^-}, q_N, p_n, q_{\bar{K}}, \cos \theta_{n\bar{K}}; M_{\pi\Sigma}) G_0(q_2, q_1) \Phi_d(q_2) d^3 q_2 \right|^2$$



Demonstration for fitting data with the 1-step $K^- d \rightarrow n K^0 "n"$ reaction calculation

- Data: $d(K^-, n)\bar{K}^0 n$ Ks/KL, BR(Ks->pi+-) corrected (K. Inoue)

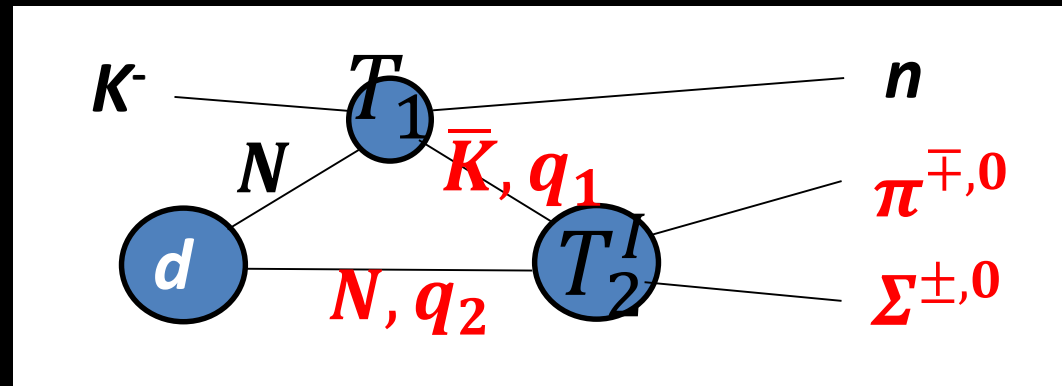


$\bar{K}N$ Scattering Amplitude

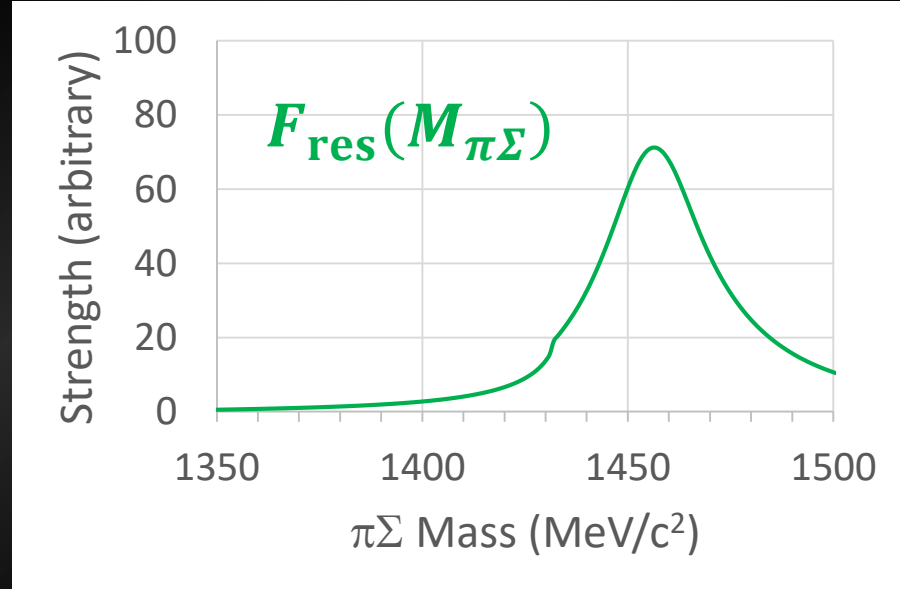
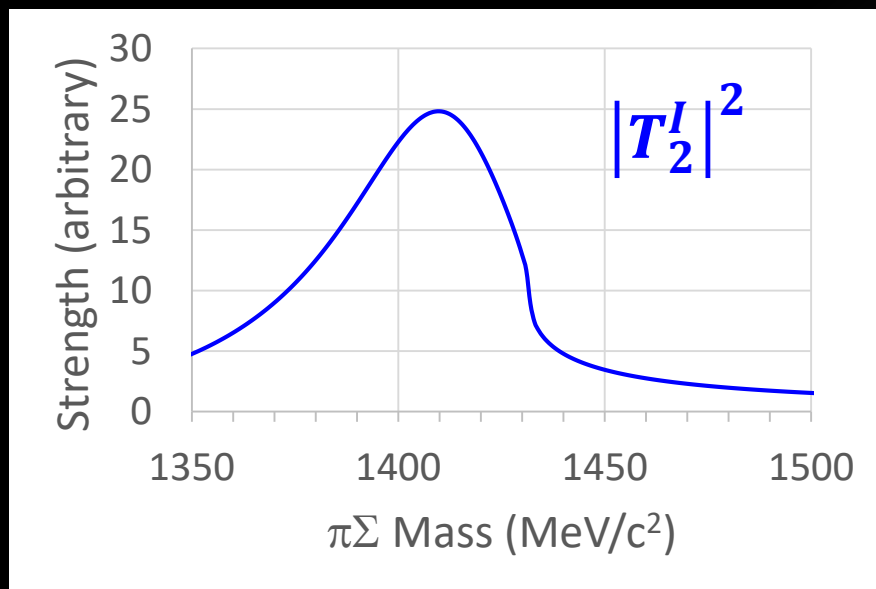
L. Lensniak, arXiv:0804.3479v1(2008)

- $T_2^I(\bar{K}N \rightarrow \bar{K}N) = \frac{A}{1-iAk_2+\frac{1}{2}ARk_2^2}$
- $T_2^I(\bar{K}N \rightarrow \pi\Sigma) = \frac{1}{\sqrt{k_1}} e^{i\delta_0} \frac{\sqrt{ImA - \frac{1}{2}|A|^2 ImR k_2^2}}{1-iAk_2+\frac{1}{2}ARk_2^2}$
- $T_2^I(\pi\Sigma \rightarrow \pi\Sigma)$
$$= \frac{e^{i\delta_0}}{k_1} \frac{\left(\sin \delta_0 + i Im(e^{-i\delta_0} A) k_2 - \frac{1}{2} Im(e^{-i\delta_0} AR) k_2^2 \right)}{1-iAk_2+\frac{1}{2}ARk_2^2}$$
- 5 real number parameters (effective range expansion)
 - A : scattering length, R : effective range, δ_0 : phase

To deduce $\bar{K}N$ scattering amplitude

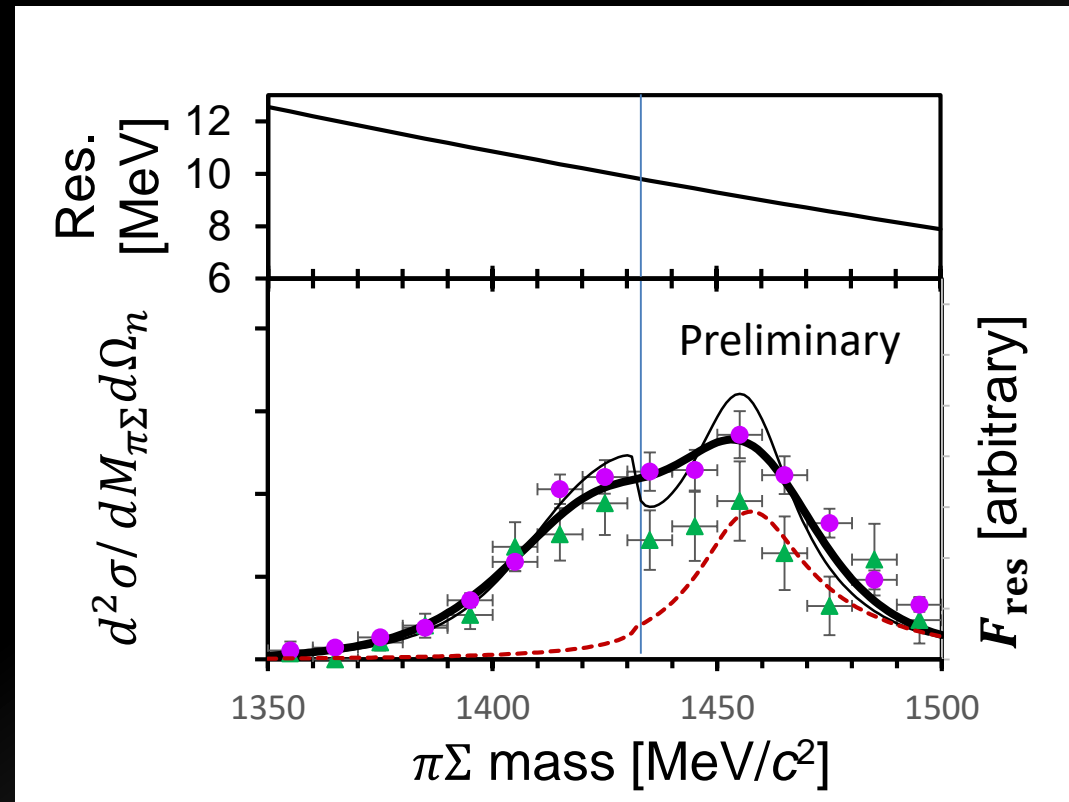


$$\frac{d\sigma}{dM_{\pi\Sigma}} \Big|_{\theta_n=0} \sim |T_2^I|^2 F_{\text{res}}(M_{\pi\Sigma})$$



$\bar{K}N$ scattering amplitude (charged+ $\pi^0\Sigma^0$)

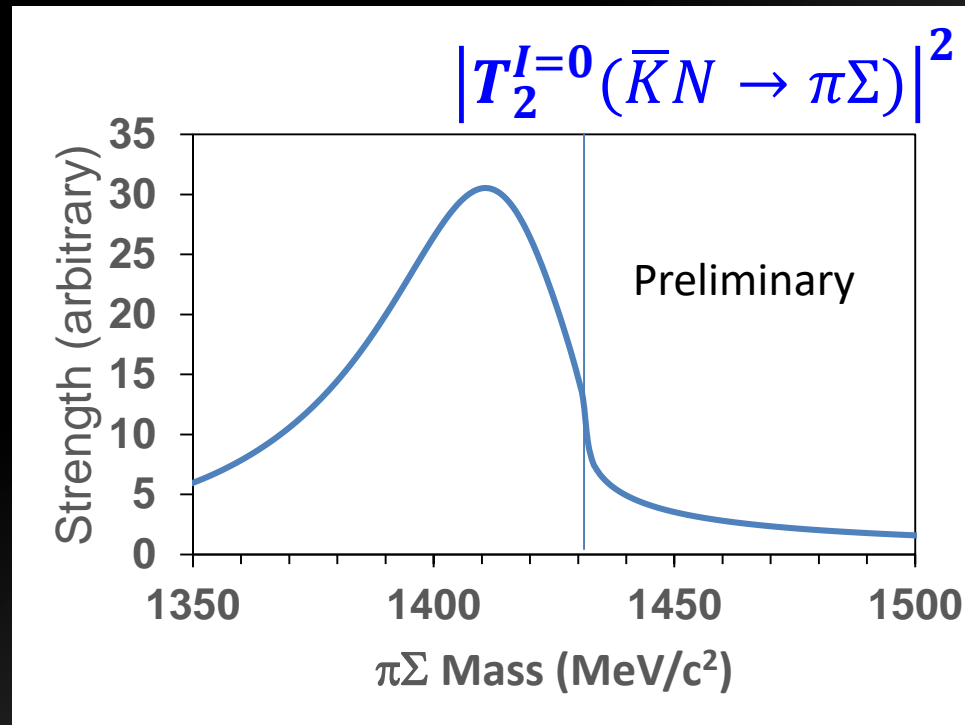
$$\frac{d\sigma}{dM_{\pi\Sigma}} \Big|_{\theta_n=0} \sim |T_2^I(\bar{K}N \rightarrow \pi\Sigma)|^2 F_{\text{res}}(M_{\pi\Sigma})$$



$\bar{K}N$ scattering amplitude (charged+ $\pi^0\Sigma^0$)

$$\frac{d\sigma}{dM_{\pi\Sigma}} \Big|_{\theta_n=0} \sim |T_2^I(\bar{K}N \rightarrow \pi\Sigma)|^2 F_{\text{res}}(M_{\pi\Sigma})$$

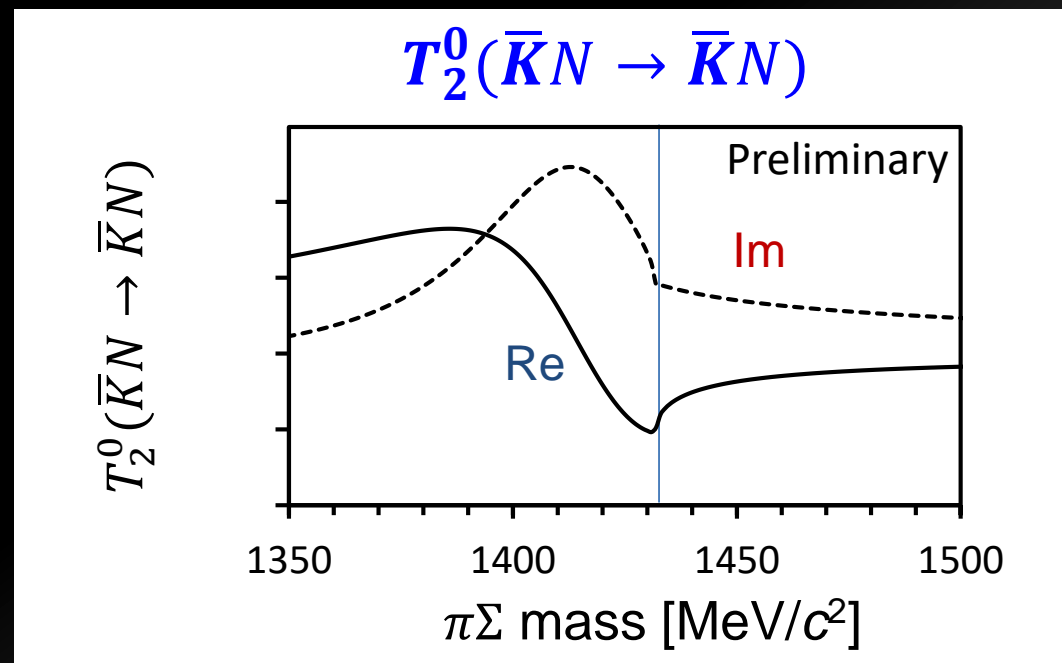
Scattering Length $A(l=0) = 0.91(0.12)$ fm
Effective Range $R(l=0) = -0.53(0.16)$ fm



$\bar{K}N$ scattering amplitude (charged+ $\pi^0\Sigma^0$)

A pole at $\sim 1416 \text{ MeV}/c^2$

$$\left|T_2^{I=0}(\bar{K}N \rightarrow \bar{K}N)\right|^2 / \left|T_2^{I=0}(\bar{K}N \rightarrow \pi\Sigma)\right|^2 \sim 1.9$$



SUMMARY

- Pole position of L(1405) seems consistent to those of the so-called higher pole suggested by the ChUM based calculations.
- The pole is likely to couple to the $\bar{K}N$ state.